https://doi.org/10.2352/lim.2024.5.1.21


# Design of a snapshot hyperspectral gonioradiometer for appearance characterization

*Nathan Slembrouck, Jan Audenaert, Frédéric B. Leloup; Light & Lighting Laboratory, KU Leuven (ESAT); Be-9000 Ghent, Belgium*

## Abstract

*Gonioradiometry plays a fundamental role in understanding the scattering properties of materials. As light interacts with surfaces, its scattering behaviour varies across different incident angles, wavelengths, and surface characteristics. Gonioradiometric measurements offer a systematic approach to quantify these intricate scattering patterns, by means of the Bidirectional Scattering Distribution function. In this paper, a new approach is presented to quantify this Bidirectional Scattering Distribution Function, for which an existing measurement instrument has been enhanced by incorporation of a hyperspectral imaging device. The hyperspectral imaging system enables detailed spectral reflectance data collection for each pixel, paving the way for measuring samples where the reflectance properties vary along the surface. Challenges such as zooming and dynamic range constraints are addressed, with the paper detailing the design and evaluation of the system. The hyperspectral gonioradiometer offers promising avenues for future research and applications in visual appearance metrology and material characterisation.*

## Introduction

By analysing how light is scattered from a sample at varying angles of incidence and detection, the complex interplay between surface texture, composition, and optical properties can be unravelled. This data is vital for visual appearance research [1], where it is used to predict subjective human perception.

A typical example of this is the measurement of optical texture, where samples show irregular reflectance across their surface. These spatial-dependant reflectance effects are typically measured with gonioradiometers utilizing cameras as their sensors. Examples of existing systems can be found at several national metrology institutes, of which a summary can be found in reference [2]. In this reference article, the devices were considered to measure sparkle, a kind of optical texture, but they could be used for other purposes as well. The gonio-spectrophotometer named GEFE at the Spanish metrology institute CSIC [3], [4] consists of a fixed illumination system powered by a Xenon broadband light source. The sample can be positioned in every possible orientation by aid of a 6-axis robot arm. METAS, the Swiss Federal Institute of Metrology, developed a multi-angle reflectance setup (MARS), which contains ten 12-bit monochrome cameras at fixed positions, together with a spectral tunable light source positioned at 3 fixed illumination directions. The Czech Metrology Institute CMI employs a system consisting of a halogen lamp, a 6-axis robot to position the sample, and an Imaging Luminance Measuring Device (ILMD) revolving around the sample. Finally, at the German metrology institute PTB, the gonio-spectrophotometer called ARGON3D makes use of either a Xenon or LED illumination source that can revolve around the sample, which in turn can be oriented by aid of a 5-axis robot. A CCD camera is used as detector in a fixed position [5].

The measurement system described in this paper resembles a similar gonioradiometer system as the ones mentioned above, but fitted with a snapshot hyperspectral camera. Hyperspectral imaging (HSI) was already used for performing colour measurements [6], [7] and research on the usefulness of these types of cameras for other aspects of visual appearance is ongoing. For example, Valero et. al. researched how a spectral tuneable camera could be used to measure effect-coatings [8]. The system achieved high accuracy, but the data capture took approximately 40 minutes. This is caused by multiple calibrations that need to be performed, as well as by using a slower spectral scanning camera.

With the faster alternative utilizing a snapshot camera, the measurement duration can be shortened. A comprehensive review of snapshot hyperspectral camera systems can be found in this study [9]. Existing infrastructure, used to measure the Bidirectional Reflectance Distribution Function (BRDF) with a spectrometer [10], was modified to carry the snapshot hyperspectral camera. The resulting HSI gonioradiometer allows the measurement of the spatially varying BRDF (svBRDF), where spatial and/or spectral irregularities in reflectance across the sample's surface are measured. In addition, the variable integration time and speed of the snapshot hyperspectral camera makes it possible to capture high dynamic range (HDR) hyperspectral images. This further improves the dynamic range and measurement quality, while the measurement duration stays shorter than three minutes.

## Design of the hyperspectral imaging gonioradiometer

The selected HSI camera is a Cubert Ultris X50. This snapshot HSI camera uses an array of 66 spectral filters with a bandwidth of 14 nm for capturing all information in one single integration period, covering a wavelength range from 350 nm to 1002 nm. The CMOS sensor is thus divided in 66 smaller bandpass wavelength regions where in each region, an image for these bandpass wavelengths is formed. Subsampling is performed automatically to obtain 164 bands. Only the bands laying in the visual spectrum are of interest to us, resulting in a remaining 102 bands. This means that 66% of the physical bands were used, resulting in 41 physical bands. No lens is needed for focussing at distances between 0.5 m and infinity. Instead, focussing is performed by correctly aligning the different wavelength images with each other, since for different distances the spatial shift between those images will differ. This principle makes the camera a lightfield camera, and focussing on a different distance can still be performed in software after taking the image, by re-aligning the wavelength images with different shifts.

The designed setup can be found in Figure 1. The hyperspectral camera was mounted on a BRDF measurement setup, which was designed by Leloup et al. An in-depth description of this BRDF device can be found in reference [10]. The setup consists of a spectrometer mounted on two axes, which allows it to rotate around a sample in both horizontal and vertical directions. The sample is illuminated by a fixed Xenon light source,

the aperture of which was enlarged to obtain a larger illuminated sample surface area, with a diameter of the illumination spot now equalling 4 cm. This unfortunately affects the homogeneity of the illumination, where a colour shift is observed towards the edges. This is not a problem however, since the setup is intended to be used for measuring reflectance using a white reference tile with known radiance factor, cancelling out the spatial variations in illumination [11].

The measurement procedure for measuring spectral reflectance (R) consists of taking two hyperspectral images: one of the reference white ($I_{ref}$), and one of the sample ($I_{sample}$). The spectral reflectance is then calculated from equation 1. Where u,v are the spatial locations of a pixel, $\lambda$ indicates the wavelength dependency, $t_{ref}$ and $t_{sample}$ indicate the integration periods for the reference and sample image, respectively, and $r_0$ is the known spectral reflectance of the white reference tile.

$$R(u,v;\lambda) = \frac{I_{sample}(u,v;\lambda)}{I_{ref}(u,v;\lambda)} \cdot \frac{t_{ref}}{t_{sample}} \cdot r_0 \quad [\%] \tag{1}$$

The worst conditions for inhomogeneous illumination occur at the edges of the spot. The spectral reflectance can be calculated under the condition that these edges still contain broadband illumination, which was verified to be true. For the left edge side, the spectral irradiance for longer wavelengths (780 nm) diminishes to about 37% of the spectral irradiance in the centre of the illumination spot. At the right edge side, the colour shift is more severe with the largest deviation occurring at shorter wavelengths (380 nm), for which the spectral irradiance reduces to 15% compared to the centre. Thus, a single exposure hyperspectral image of these edges would result in more noise in these regions because of the lower signal strength. This can be countered by using HDR imaging.

The biggest challenge when mounting the hyperspectral camera onto the gonioradiometer is focussing on distances closer than 0.5 m in order to enhance the spatial resolution. The spatial resolution can be calculated as the ratio between the image height and the number of pixels. At an image distance of 0.5 m from a sample, the spatial resolution at the sample plane would equal 553 µm, which is insufficient to register detailed spatial information like small texture and colour variations within the sample. An example of this can be found in the evaluation section. Therefore, a convex lens with a measured focal length of 18.8 cm is placed in front of the camera. Now, objects laying at a distance of 18.8 cm result in parallel rays travelling towards the camera. By focussing the camera at infinity, a sharp image is formed with a spatial resolution of 208 µm. Using the thin lens equation with a focal length (f) of 18.8 cm and an image distance ($z_i$) of 50 cm, the resulting minimal object distance equals 13.6 cm. At this distance, the spatial resolution equals 143 µm. The ray diagram and relationship between the image distance ($z_i$) and object distance ($z_o$) is presented in Figure 2.

As explained earlier, the filter array captures 66 different images on different locations of the sensor. The lens must be larger than the size of the filter array to deliver a sharp image for each wavelength. However, the use of a single lens limits the amount of zoom that can be used. The camera and lens cannot be located too close to the sample, otherwise the collimated light beam would get blocked by the camera. The selected lens has a diameter of 8.7 cm, which unfortunately causes an obstruction angle of approximately 25°. The addition of this lens already improves the spatial resolution significantly, but alternative systems summarized in the introduction still achieve better results with resolutions ranging between 24 µm and 45 µm. Therefore,

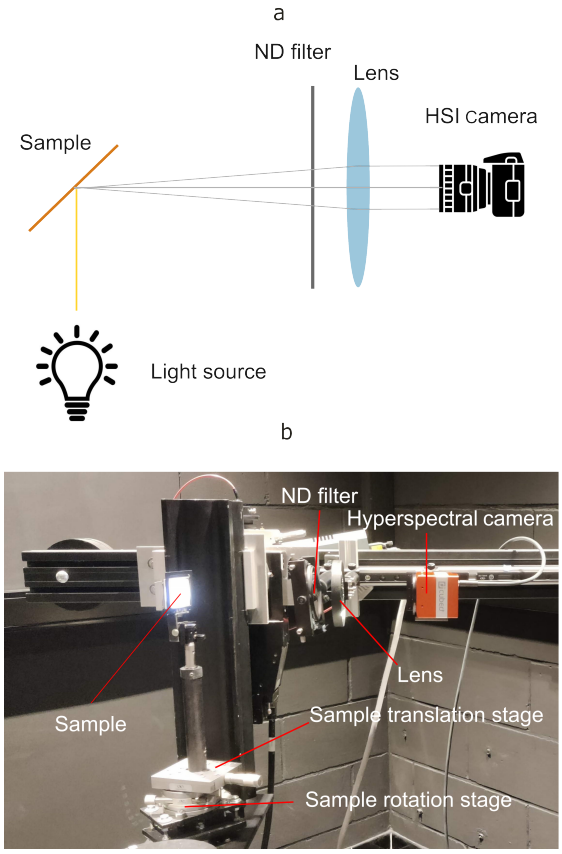


***Figure 1.*** *Schematic and image of the HSI gonioradiometer*

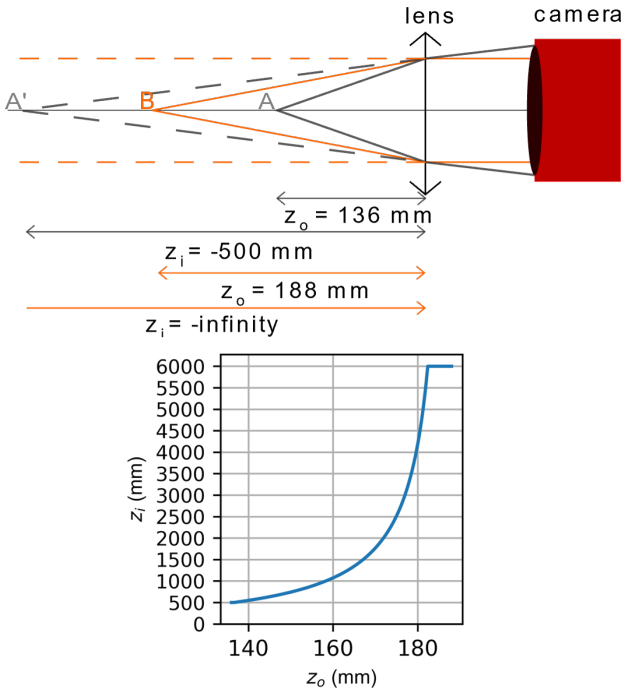


***Figure 2.*** *Upper: ray diagram for the convex lens with a focal length of 188 mm. Object A is located at 136 mm and A' represents its image. Object B is stood at a distance of 188 mm from the lens, with its image laying at infinity. Lower: distance relationship for the convex lens, calculated with the thin lens equation. When focussing the camera, a calibration distance $z_i$ will focus on an object at distance $z_o$*

measuring sparkle would require a better zooming system. Nevertheless, specific visual appearance attributes that do not require this small spatial resolution, can now be measured. One such example is the measurement of orange peel [12].

By introducing a lens to enhance the spatial resolution, an undesirable effect occurs. The spectral filters used by the hyperspectral camera are reflective filters, which would not be problematic if the sample were to be located at a large distance. However, at close distances, a large amount of straylight reflects back onto the sample. These reflections compromise the otherwise strong directional illumination, and cannot be filtered out in software since in general, the measured samples have different scatter patterns than the white calibration tile. An example of the undesired reflections can be seen in Figure 3, where these were reduced by introduction of an absorbing neutral density (ND) filter in front of the hyperspectral camera and the lens. Calculated from the plots in Figure 3, the oscillations caused by the filters are now reduced with an average factor of three. Even though the ND filter is an absorbing type as opposed to a reflective type, it was tilted to avoid Fresnel reflections occurring at both sides of the filter (towards the camera and towards the sample). While reducing the useful amount of light reaching the hyperspectral camera, this solution is feasible because the snapshot hyperspectral camera can capture low light scenes still relatively fast, in less than 5 seconds. For many slower types of hyperspectral cameras, this solution would make the measurement times too long for capturing a high amount of illumination/viewing geometries in one session.

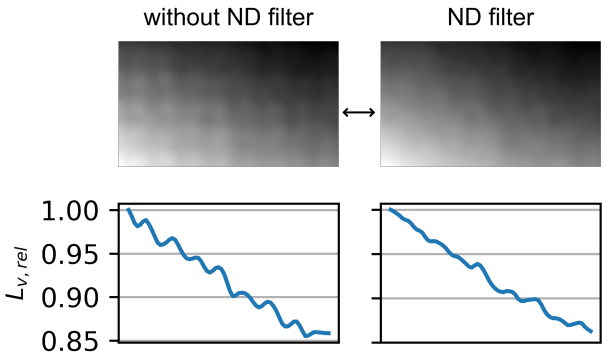


***Figure 3.*** *Effect of adding an ND filter, shown on a cropped relative luminance image constructed from the hyperspectral datacube. The plots below show a horizontal cross-section of the relative luminance images at the position indicated by the double arrow.*

## HDR

The camera has 12-bit depth and the integration time ranges from 0.1 milliseconds to 10 seconds. An HDR algorithm was implemented in order to cover a larger dynamic range. The HDR algorithm starts at the highest integration time and halves it with each step, ensuring that every pixel reports at least 50% of the maximum value for one of the hyperspectral images in the HDR series. Reconstruction of the hyperspectral image is performed by, per pixel and per specific wavelength, using the highest value from the HDR series which is not yet saturated and dividing it by its specific integration time. In practice, the HDR algorithm started with an integration time of 5 seconds and stopped at 1 millisecond, which takes 13 steps. Linearity for this series of integration times was checked by performing an HDR measurement on a Gretag Macbeth® chart for longer integration times (200 ms – 5000 ms), while for shorter integration times an image of a halogen light source behind a diffuser was used. The correlation coefficient between integration time and sensor count $R^2$ is 0.9999, indicating excellent linearity. In addition, linearity of the quantization was checked by using a dimmable LED and the camera set at a fixed integration time of 80 ms. The correlation between measured illuminance and sensor count again numbered 0.9999. The framerate for a single exposure image is set to 0.1Hz, including the acquisition time. Therefore, considering there are 13 different acquisitions in the HDR algorithm, one HDR capture takes 130 seconds.

## Validation

Previous research already compared the Gretag Macbeth® measurements of the hyperspectral camera against three other spectral measurement devices, indicating acceptable correlations [13]. Now, measurements of the presented HSI gonioradiometer are compared to measurements performed with a portable spectrophotometer (Xrite MA-T6), that was also used in this previous paper. A total of 12 Gretag Macbeth® patches were measured under a measurement geometry of 45°:0° (illumination:viewing). A mean CIEDE2000 colour difference for the 12 patches of 1.01 indicates a barely noticeable colour difference, and slightly improves on the CIEDE2000 of 1.13 that was measured in our previous research. Therefore, it is concluded that the addition of the lens and ND filter did not negatively influence the spectral precision of the camera. As an example, three measured Gretag Macbeth® spectra are presented in Figure 4, and a more detailed evaluation of the precision for the 12 patches is reported in Table 1. From Figure 4, it can be observed that the spectral reflectance for short wavelengths (400 nm) measures too high. This is the result of the white reference tile used, which does not have high spectral reflectance in the short wavelength region. This could be fixed by using a higher quality reference white tile, like spectralon® for example.

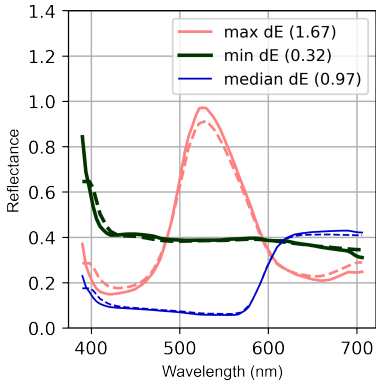


***Figure 4.*** *Three of the measured Macbeth patches, continuous functions are measurements from the HSI gonioradiometer, dotted functions are measurements from the Xrite MA-T6*

**Table 2 - Metrics for comparing the setup with the Xrite MA-T6**

| metrics | GFC | MAE [%] | NMRSD [%] | DE2000 |
|---|---|---|---|---|
| mean | 0.9993 | 1.7137 | 4.6229 | 1.0094 |
| median | 0.9996 | 1.8612 | 4.8723 | 0.9745 |
| st. dev. | 0.0006 | 0.7380 | 2.6765 | 0.4269 |
| max | 0.9999 | 3.3980 | 10.6368 | 1.6692 |
| min | 0.9982 | 0.7715 | 1.2682 | 0.3184 |

The added value of the HDR algorithm is also illustrated by measuring the Gretag Macbeth® chart, for which measurements with and without HDR were again compared against the measurements of the Xrite MA-T6. These measurements were performed on the whole Gretag Macbeth® chart (24 patches) without mounting the camera on the gonioradiometer, because a much larger illuminated surface area (420 mm x 594 mm) is required when measuring all patches at once. Instead, a halogen light source was used under 45° with the chart, and the camera stood 0.5 m perpendicular from the chart. This setup gives worse correlations with measurements from the Xrite MA-T6 because the halogen light source emits less blue light, but the relative improvement when using HDR can still be examined. First, a series of 20 hyperspectral images with the same integration time is averaged to examine whether simple averaging could be beneficial. The mean CIEDE2000 colour difference for the 24 patches when averaging the 20 hyperspectral images is 2.64. When calculating the mean colour difference of the 24 patches for each hyperspectral image in the series of 20, the lowest mean colour difference is 2.57 (97% of 2.64) and the highest mean colour difference is 2.78 (106% of 2.64). This means that there is a small advantage for averaging images with the same exposure. When using HDR, the mean colour difference for the 24 patches reduces to 1.78. The same metrics used in Table 1 were all checked, and they all showed similar improvements. This result shows that the spectral precision improves significantly when HDR is used.

As a practical example, the HSI gonioradiometer was used to measure the reflectance characteristics of a laminate floor. This laminate was made to imitate the appearance of African padauk wood, of which the appearance was researched in [14]. This is a type of wood that shows the effect of “ribbon strip” or “strip figure”, which is a gonio-apparent effect where the stripes can quickly become darker or brighter under small rotations, giving the wood a very dynamic appearance. The laminate imitates this appearance by a printed pattern that mimics grain direction and annual growth rings of the wood. In addition, a finishing layer enhances the glossiness and a structure is pressed into to surface to evoke roughness. In Figure 5, a picture is shown of the laminate tile, next to an illustration of the wood’s structure.

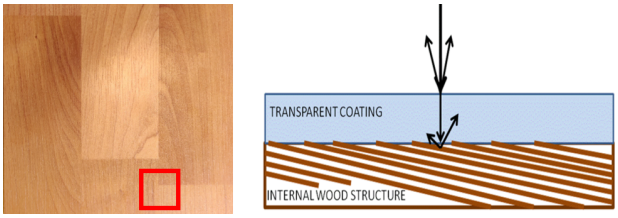


***Figure 5.*** *Preview image of the laminate tile, with the red square indicating the measured zone, and an illustration of the structure of padauk wood. When viewed from the right of the illustration, the wood will appear brighter than when viewed from the left.*

The measurement was performed under a measuring geometry of 45°:0°. The results can be found in Figure 6 , where it has been compared to a measurement performed without the added lens where the camera stood at 0.5 m from the sample. It is clear that without the lens, the wood’s fine structure cannot be seen. Figure 6.b shows the relative intensities across the sample (cross section indicated by the red line in Figure 6.a). This shows that the setup without the lens would show too high reflectances for darker spots on the sample, and lower reflectances for brighter spots of the sample. Figure 6.c plots the reflectance spectrum of one such local brighter spot and one local darker spot. The dark spot is indicated by a blue square on the preview images, the bright spot by a green square.

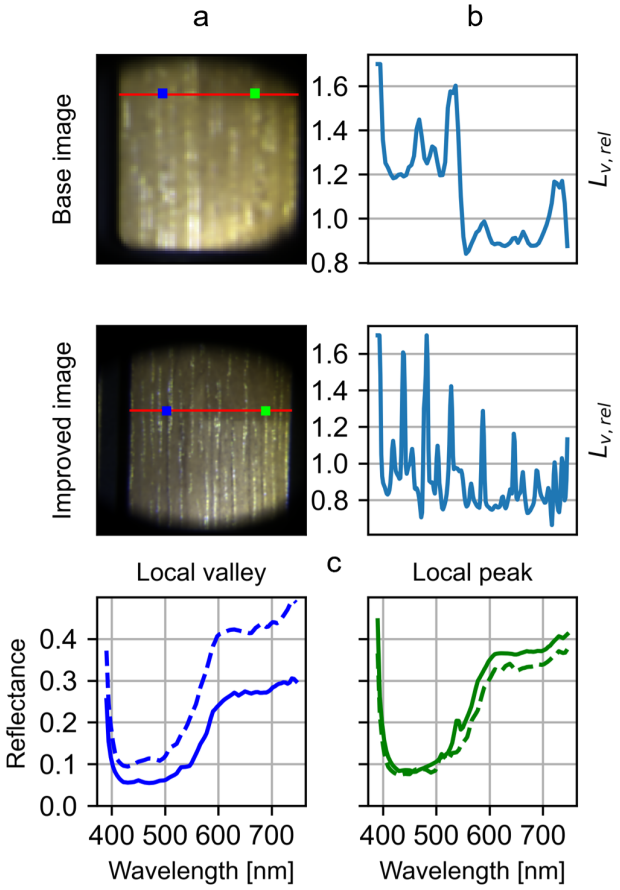


***Figure 6.*** *Measurement of a laminate floor tile with and without the added lens. Part a displays the preview image, part b plots the relative luminance of a cross section and part c plots one example of a darker pixel (local valley) and on example of a bright pixel (local peak).*

## Discussion and Conclusion

A new HSI gonioradiometer was designed and verified, intended to be used for measuring spectral reflectance properties and their variation between different locations of non-uniform samples. Using a snapshot hyperspectral camera, the measurements can be performed quickly and with high dynamic range. A lens was introduced to improve the spatial resolution, and an ND filter minimizes the amount of light reflected back towards the sample.

The system still needs some improvements in the future. To enhance spatial resolution, a basic convex lens was initially employed. However, using more advanced optical systems with stronger zoom capabilities would improve the measurement of spatial details even more. In addition, the camera could then be placed further from the camera, increasing the angular resolution. The setup could then be used to measure several properties like colour homogeneity, optical texture effects, and transmittance properties.

## References


[1] M. 'Pointer, M. 'Brill, J. 'Veitch, P. 'Bodrogi, E. 'Burini, J. 'Campos, A. 'Chalmers, S. 'Cheung, P. 'Clarke, O. 'da Pos, and G. 'Derefeldt, *A framework for the measurement of visual appearance*. CIE, 2006. [Online]. Available: https://cie.co.at/publications/framework-measurement-visual-appearance

[2] A. Ferrero, N. Basic, J. Campos, M. Pastuschek, E. Perales, G. Porrovecchio, M. Šmid, A. Schirmacher, J. L. Velázquez, and F. M. Martínez-Verdú, "An insight into the present capabilities of national metrology institutes for measuring sparkle," *Metrologia*, vol. 57, 12 2020.

[3] A. M. Rabal, A. Ferrero, J. Campos, J. L. Fontecha, A. Pons, A. M. Rubīo, and A. Corróns, "Automatic goniospectrophotometer for the absolute measurement of the spectral brdf at in- and out-of-plane and retroreflection geometries," *Metrologia*, vol. 49, pp. 213–223, 6 2012.

[4] B. 'Bernad, A. 'Ferrero, A. 'Pons, M. L. 'Hernanz, and J. C. Acosta, "Upgrade of goniospectrophtometer gefe for near-field scattering and fluorescence radiance measurements," in *Proc. SPIE 9398*. SPIE, 3 2015.

[5] A. Höpe, T. Atamas, D. Hünerhoff, S. Teichert, and K.-O. Hauer, "Argon3: "3d appearance robot-based gonioreflectometer" at ptb," *Review of Scientific Instruments*, vol. 83, 4 2012.

[6] F. Cherubini, A. Casini, C. Cucci, M. Picollo, and L. Stefani, "Application of a hyperspectral camera for colorimetric measurements on polychrome surfaces in a controlled environment and evaluation of three image processing software for displaying colorimetric data: Pros and cons of the methodology presented," *Color Research and Application*, 3 2022.

[7] A. Raza, D. Dumortier, S. Jost-Boissard, C. Cauwerts, and M. Dubail, "Accuracy of hyperspectral imaging systems for color and lighting research," *LEUKOS - Journal of Illuminating Engineering Society of North America*, vol. 19, pp. 16–34, 2023.

[8] E. M. Valero, M. A. Martínez, E. Kirchner, I. van der Lans, M. García-Fernández, T. Eckhard, and R. Huertas, "Framework proposal for high-resolution spectral image acquisition of effect-coatings," *Measurement: Journal of the International Measurement Confederation*, vol. 145, pp. 379–390, 10 2019.

[9] N. Hagen and M. W. Kudenov, "Review of snapshot spectral imaging technologies," *Optical Engineering*, vol. 52, p. 090901, 9 2013.

[10] F. B. Leloup, S. Forment, P. Dutré, M. R. Pointer, and P. Hanselaer, "Design of an instrument for measuring the spectral bidirectional scatter distribution function," *Applied Optics*, vol. 47, p. 5454, 10 2008. [Online]. Available: https://opg.optica.org/abstract.cfm?URI=ao-47-29-5454

[11] D. H. Foster and K. Amano, "Hyperspectral imaging in color vision research: tutorial," *Journal of the Optical Society of America A*, vol. 36, p. 606, 4 2019.

[12] T. Sone and S. Watanabe, "Measurement and evaluation method of orange peel," in *IS and T International Symposium on Electronic Imaging Science and Technology*. Society for Imaging Science and Technology, 2017, pp. 62–65.

[13] N. Slembrouck, F. Leloup, and J. Audenaert, "Snapshot and linescan hyperspectral imaging for visual appearance measurements," in *CIE x050:2023 Proceedings of the 30th Session of the CIE, Ljubljana, Slovenia, September 15 – 23, 2023, Volume 1*. International Commission on Illumination, CIE, 12 2023, pp. 1227–1236.

[14] F. B. Leloup, M. R. Pointer, P. Dutré, and P. Hanselaer, "characterization of stripe figure on finished wood," in *Proc. AIC*. AIC, 2009.


## Author Biography

*Nathan Slembrouck is a PhD researcher at the Light & Lighting Laboratory of KU Leuven. He received his masters degree in electronical engineering technology from KU Leuven in 2022. His main research topic covers image-based appearance metrology, where the design of new measurement instruments and psychophysical appearance experiments are combined.*

*Jan Audenaert graduated as a master in information and communication technology from Katholieke Hogeschool (KAHO) Sint- Lieven (Gent) in 2009. He obtained his PhD in engineering from KU Leuven in 2014. Currently he is active at the Light & Lighting Laboratory as a research expert with a main research focus on ray tracing for non-imaging optics and near-field goniophotometry.*

*Frédéric Leloup received his MSc in Electromechanical Engineering in 2001 and PhD in Engineering in 2012, both from KU Leuven (Belgium). He worked as a research fellow and postdoc researcher at the Light & Lighting Laboratory research group, before being appointed associate professor in the Department of Electrical Engineering at KU Leuven in 2022. His research focuses on hard and soft lighting metrology. Frédéric is president of the Belgian Institute on Illumination and National Representative within CIE Division 1 (Vision and Colour).*